Computers, Materials & Continua CMC, vol.61, no.1, pp.141-154, 2019

Development of an Ultrasonic Nomogram for Preoperative Prediction of Castleman Disease Pathological Type

Xinfang Wang[1], Lianqing Hong[2], Xi Wu[3], Jia He[3], Ting Wang[3, 4, *], Hongbo Li[5] and Shaoling Liu[6]

Abstract: An ultrasonic nomogram was developed for preoperative prediction of Castleman disease (CD) pathological type (hyaline vascular (HV) or plasma cell (PC) variant) to improve the understanding and diagnostic accuracy of ultrasound for this disease. Fifty cases of CD confirmed by pathology were gathered from January 2012 to October 2018 from three hospitals. A grayscale ultrasound image of each patient was collected and processed. First, the region of interest of each gray ultrasound image was manually segmented using a process that was guided and calibrated by radiologists who have been engaged in imaging diagnosis for more than 5 years. In addition, the clinical characteristics and other ultrasonic features extracted from the color Doppler and spectral Doppler ultrasound images were also selected. Second, the chi-square test was used to select and reduce features. Third, a naïve Bayesian model was used as a classifier. Last, clinical cases with gray ultrasound image datasets from the hospital were used to test the performance of our proposed method. Among these patients, 31 patients (18 patients with HV and 13 patients with PC) were used to build a training set for the predictive model and 19 (11 patients with HV and 8 patients with PC) were used for the test set. From the set, 584 high-throughput and quantitative image features, such as mass shape size, intensity, texture characteristics, and wavelet characteristics, were extracted, and then 152 images features were selected. Comparing the radiomics classification results with the pathological results, the accuracy rate, sensitivity, and specificity were 84.2%, 90.1%, and 87.5%, respectively. The experimental results show that radiomics was valuable for the differentiation of CD pathological type.

Keywords: Radiomics, ultrasonic nomogram, Castleman disease, Bayesian, feature extraction.

[1] Ultrasound Department of Nanjing Integrated Traditional Chinese and Western Medicine Hospital Affiliated with Nanjing University of Chinese Medicine, Nanjing, 210014, China.

[2] Pathology Department of Nanjing Integrated Traditional Chinese and Western Medicine Hospital Affiliated with Nanjing University of Chinese Medicine, Nanjing, 210014, China.

[3] Department of Computer Science, Chengdu University of Information Technology, Chengdu, 610225, China.

[4] Vanderbilt University Institute of Imaging Science, Nashville, TN, 37232, USA.

[5] Ultrasound Department of Affiliated Hospital of Nanjing University of Chinese Medicine, Nanjing, 210029, China.

[6] Ultrasound Department of Shandong Provincial Medical Imaging Research Institute, Jinan, 250021, China.

[*] Corresponding Author: Ting Wang. Email: wangtingscu@126.com.

1 Introduction

Castleman disease (CD) is a rare chronic lymphoproliferative disorder that was first reported and named by Dr. Benjamin Castleman in 1956. It is known as giant lymph node hyperplasia or vascular follicular lymphoid tissue hyperplasia because of its manifestation of massive lymphadenopathy, and vascular and follicular hyperplasia. The incidence of this disease is low, and the current reports of the disease in the literature are mostly case and group cases.

Clinically, CD is classified into unicentric CD (UCD) and multicentric CD (MCD), depending on the distribution of enlarged lymph nodes and organ involvement. The former has a relatively high incidence rate and often occurs in people aged 20-30 years, involving a single lymph node area, with mild symptoms and good prognosis; the latter has a relatively low incidence rate (approximately 1/5 of the annual new CD cases in the United States are MCD), often occurs in the 40-60-year-old population, can involve multiple lymph node areas and the liver, lung, kidney, and other important organs, and exhibits more systemic symptoms and poor prognosis, with a 5-year mortality rate up to 35% [Ma and He (2013)].

The diagnosis of CD depends on pathology. The main pathological types include hyaline vascular variant, plasma cell variant, and mixed variant (histopathologically, HV, PC, and MIX). The common pathological features of CD are that the basic structure of the lymph nodes remains intact, the lymphoid follicles proliferate, and there is a large number of degenerated capillaries between follicles. The main feature of HV-CD is that there are multiple layers of circularly arranged lymphocytes around the follicles, forming a unique onion skin-like structure. PC-CD is characterized by a large number of mature plasma cells in the follicular stroma, lymphocyte proliferation around the follicles, and far less capillary proliferation between the follicles compared to HV, with generally no typical onion-like structure. MIX-CD exhibits both characteristics or a component [Soumerai, Sohani and Abramson (2014)].

Frizzera [Frizzera (1988)] proposed the diagnostic criteria for CD. (1) UCD diagnostic criteria: single site lymphadenopathy, histopathological features of hyperplasia, except for other primary diseases, no systemic symptoms or anemia, elevated immunoglobulin, (except for PC), long-term survival after tumor resection; (2) MCD diagnostic criteria: characteristic histopathological changes, significant lymphadenopathy involving multiple peripheral lymph nodes, and multiple system involvement, excluding other causes. Since the disease occurs at different sites, clinical manifestations are diversified, clinical symptoms are not specific, and preoperative diagnosis is difficult. Preoperative ultrasound (US) examination is helpful for establishing a CD diagnosis.

The early diagnosis of this disease ultimately depends on histopathological examination. For CD, regardless of the clinical or pathological classification, there are common features of histology: (1) an intact lymph node basic structure; (2) lymphoid follicles and vascular proliferation, in transparent vascular follicles, angiogenesis, glassy changes, atrophy of follicular germinal centers; PC-CD shows more plasma cells in the follicular stroma, with follicular germinal center hyperplasia [Bucher, Chassot, Zufferey et al. (2005); Nu, Liu and Diss (2001); Xuan (2015); Zhang, Wang and Dong (2008)]. Preoperative knowledge of CD can provide valuable information for determining the need for adjuvant therapy and

the adequacy of surgical resection, thus aiding in pretreatment decision making.

In recent years, with the rapid advancement of imaging equipment and imaging technology, US has become an important imaging tool for endocrinologists and surgeons to use for establishing a CD diagnosis. US has the outstanding advantages of high resolution, low damage, high cost effectiveness, and high convenience for soft tissues, and has become the best choice for identifying the manifestation of mass [Hacihaliloglu (2017)]. Studies have shown that US has a great advantage in identifying lymphadenopathy, and vascular and follicular hyperplasia, because there are significant differences in the size, shape, number, cystic change, calcification, blood supply, and other aspects of mass in US images. Therefore, clinicians can identify the manifestation of mass based on these characteristics. However, it should be noted that none of the US features are unique to CD, and therefore, a comprehensive analysis is required to make a correct diagnosis of CD pathological type. Furthermore, because there are no unique clinical symptoms of CD, the diagnosis should be combined with the patient's age, gender, medical history, physical signs, and other information as well as various examinations for comprehensive analysis. The complex diagnostic indicators increase the difficulty in arriving at a correct diagnosis. In addition, US images are mostly noisy, image quality is not clear, and organs are blurred. Therefore, the above factors have a great impact on the diagnostic accuracy of the CD pathological type. Without the biopsy, different physicians may make different assessments from the same image.

With the development of science and technology, computer-aided diagnosis is becoming more widely used in medical research. The concept of radiomics was proposed by Lambin et al. [Lambin, Rios-Velazquez, Leijenaar et al. (2012)] in 2012 and is defined as the high-throughput extraction of a large number of advanced quantitative imaging features from radiographic images and analysis. The computer extracts and analyzes the US image information to assist with solving the problems in US diagnosis.

To the best of our knowledge, there is no study that has determined whether a radiomics signature would enable superior prediction of CD pathological type. Therefore, the aim of the present study was to develop an ultrasonic nomogram that incorporated both the radiomics signature and clinicopathologic risk factors for individual preoperative prediction of CD pathological type.

2 Materials and methods

2.1 Patients

Ethical approval was obtained for this analysis. All of the participants provided written informed consent as approved by the Institutional Review Board of Nanjing Hospital of Integrated Traditional Chinese and Western Medicine. Fifty cases of CD confirmed by pathology from January 2012 to October 2018 from three hospitals (Nanjing Hospital of Integrated Traditional Chinese and Western Medicine, Affiliated Hospital of Nanjing University of Chinese Medicine, and Shandong Provincial Medical Imaging Research Institute) were collected, including 23 males and 27 females, aged 23 to 59 years old. Among these patients, 31 patients were used to build a training set for the predictive model and 19 for the test set. The training set included 18 patients with HV and 13 patients with PC. There were 11 cases of HV in the test group and 8 cases of PC.

2.2 Ultrasound image acquisition

All of the participants underwent US scanning. GE Voluson E8, Philips EPIQ5, Siemens 300 color ultrasonic diagnostic equipment was used. We did not control for probe type. The patients fully exposed the site to be examined in a supine position. The direct examination method was adopted, and the probe coated with the coupling agent was directly detected in the lesion. Three US imaging techniques (gray-scale ultrasound, color Doppler ultrasound (CDFI), and spectral Doppler (PW)) were performed for each participant.

Two experienced radiologists independently examined all of the images in the CD dataset and were blinded to the biopsy results. Each radiologist chose an image from each patient's series of images that best displayed the mass echo-texture. On that image, each drew an area designated the region of interest (ROI) using ImageJ software [Schneider, Rasband and Eliceiri (2012)]. They were not specifically looking for CD or its absence, but rather, just the image and region in the image that most clearly demonstrated the mass texture. The ROIs also accounted somewhat for depth distortion from the US, as the radiologists designated ROIs at a depth approximating the focal length of the scan.

2.3 Gray ultrasound image segmentation

The data set was provided by the medical US department in DCM format. To facilitate image segmentation, it was necessary to convert the data in DCM format into BMP format. To extract the image characteristics of the relatively accurate mass area, each US image mass area was calibrated by a physician with extensive experience in CD US, and then the ROI was segmented using Adobe Photoshop CC2017 and MATLAB R2016b software. Fig. 1 shows gray US image of a HV-CD case and the corresponding segmentation result.

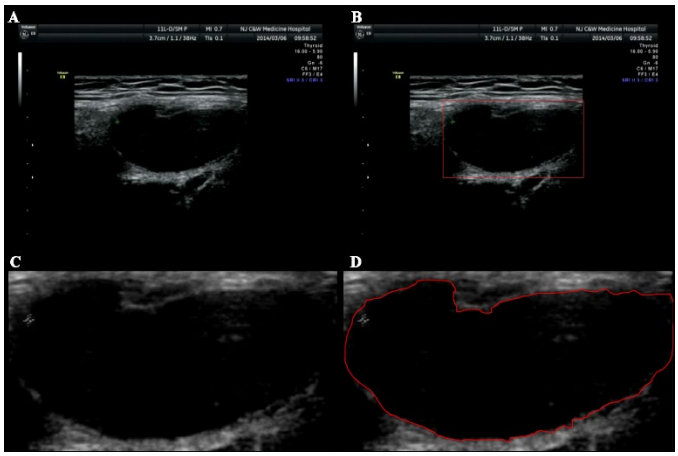

Figure 1: (A) HV-CD ultrasound original image; (B) HV-CD mass ROI; (C-D) HV-CD segmentation and edge-labeled results

2.4 Feature extraction

The key step in radiomics is to extract high-dimensional feature data for quantitative

analysis of ROI attributes. Subsequent classifier prediction results depend on the features used, which requires a feature extraction method that is highly reusable and contains sufficient information. The quantitative image features extracted in this study can be divided into five categories, including:

(1) Intensity features

Converts data into a single histogram based on the intensity characteristics of the histogram. Commonly used statistical values can be calculated by histograms. The intensity features extracted in this study include first-order statistical features, such as kurtosis, maximum value, minimum value, skewness, and entropy.

(2) Shape and size characteristics

The shape and size features extracted herein include surface area, volume, tightness, surface area-to-volume ratio, and sphericity. Surface area and volume provide information on the size of the mass. Mass compactness, surface area-to-volume ratio, and sphericity describe the shape characteristics of the mass, such as whether the shape is close to a sphere, a circle, or an elongated strip. The sphericity is the degree to which the shape of the mass is close to a sphere.

(3) Texture features

Texture features can be used to quantify differences in heterogeneity within the mass. Second-order statistics or co-occurrence matrices can be used for texture classification in medical pattern recognition. The texture features usually include a gray level co-occurrence matrix (glcm), a gray level run length matrix (glrlm), and a gray level size matrix (glszm). There are multiple gray level size zone matrix (mglszm) features. The gray level co-occurrence matrix describes the texture via the spatial characteristics of the gray scale. A gray level co-occurrence matrix can be obtained due to the fact that two pixels at a certain distance in the image have a certain gray level. The swim length matrix quantizes the gray level run of an image.

(4) Wavelet features

The wavelet feature extracted in this study is a first-order statistical feature and texture feature of the original image under wavelet decomposition.

(5) Other features

Other features included location, number, hilum of the lymph gland, internal echo, blood flow type, blood flow grading, and resistance index (RI) value of the mass. In addition, clinical characteristics of patients were collected, including the gender, age, and disease duration.

Based on the above feature extraction method, a total of 584 quantitative image features were extracted.

2.5 Feature selection and dimensionality reduction

Correlation and redundancy between features will reduce the accuracy of classification. At the same time, medical images usually belong to small sample learning. Too many features will increase the complexity of the classifier, cause over-fitting, and reduce the generalization ability of the classifier. Therefore, it is necessary to select and reduce the dimensions of the feature set.

Feature selection is the selection of a feature subset from all feature spaces, so that the model constructed with the selected feature subset is more optimal. The feature selection method adopted in this study is based on the filter feature selection of the chi-square test. The chi-square test is a widely used hypothesis test method, especially in classification data statistics. Chi-square statistics can measure the closeness of the relationship between variables. In the current study, a score was calculated for each feature, that is, the chi-square statistic, and 152 features with higher scores were selected to participate in the dimension reduction of subsequent features.

After the chi-square test, the possible interdependencies between features are ignored by the variable ordering method. In the current study, the principal component analysis (PCA) dimensionality reduction method was used to synthesize the high-dimensional variables that may be correlated to synthesize linearly independent low-dimensional variables, which solves the above problems. The difference between feature selection and feature dimension reduction is that dimension reduction essentially maps from one dimension space to another, the dimension decreases, and the eigenvalue changes. The feature after feature selection is only the child of the original feature. In a set, the dimension is reduced but the eigenvalue is unchanged.

2.6 Ultrasonic nomogram building

Using the features after feature selection and dimension reduction, the CD pathological classification prediction model was trained by a Gaussian Bayesian model and predicted by the prediction model using the test set.

The Gaussian Naïve Bayesian method is a set of supervised learning algorithms based on Bayes' theorem, and requires each pair of features to be independent of each other. Given a category y and a related feature vector from x_i to x_n, the relationship is obtained by Bayes' theorem.

$$P(\mathrm{y}|x_1,\cdots,x_n)=\frac{P(y)P(x_1,\cdots,x_n|y)}{P(x_1,\cdots,x_n)} \tag{1}$$

Assume that each pair of features is independent of each other,

$$P(x_i|y,x_1,\cdots,x_{i-1},x_{i+1},\cdots,x_n)=\mathrm{P}(x_i|\mathrm{y}) \tag{2}$$

Obtained by Equations (1) and (2),

$$P(\mathrm{y}|x_1,\cdots,x_n)=\frac{P(y)\prod_{i=1}^{n}P(x_i|y)}{P(x_1,\cdots,x_n)} \tag{3}$$

Since $\mathrm{P}(x_1,\cdots,x_n)$ is a normalized constant, the classification rules:

$$P(\mathrm{y}|x_1,\cdots,x_n)\propto \mathrm{P}(\mathrm{y})\prod_{i=1}^{n}P(x_i|y) \tag{4}$$

which can be:

$$\hat{y}=\arg\max_{y}P(y)\prod_{i=1}^{n}P(x_i|y) \tag{5}$$

Finally, $\mathrm{P}(\mathrm{y})$ and $\mathrm{P}(x_i|\mathrm{y})$ are estimated using Maximum A Posteriori (MAP); the former is the relative frequency of the category y in the training set.

The difference between Naïve Bayes comes from the different assumptions made when dealing with $\mathrm{P}(x_i|\mathrm{y})$ distribution. This study uses the Gaussian Naïve Bayes method,

assuming that $P(x_i|y)$ obeys Gaussian distribution.

$$P(x_i|y) = \frac{1}{\sqrt{2\pi\sigma_y^2}} exp\left(-\frac{(x_i-\mu_y)^2}{2\sigma_y^2}\right) \quad (6)$$

Thus, the value of $P(x_i|y)$ in each class is calculated, and the classification result is obtained by comparing the sizes.

3 Results

3.1 Clinical characteristics

Patient characteristics in the primary and validation cohorts are given in Tab. 1. There are no significant differences between the two cohorts in age, or gender. HV-CD accounts for approximately 58.1% and 57.9% in the primary and validation cohorts, respectively.

Table 1: Characteristics of patients in the primary and validation cohorts

Characteristic	Primary cohort			Validation cohort		
	HV	PC	P	HV	PC	P
number	18	13	-	11	8	-
Age (years, mean±SD)	39.24±8.88	37.44±8.57	0.329	41.8±7.72	44.87±7.41	0.151
Gender (male\female)	8\10	6\7	0.925[a]	5\6	4\4	0.845[a]
RI	0.57±0.05	0.58±0.05	0.529	0.58±0.05	0.57±0.06	0.611

[a] Fisher's exact test. P value was derived from the univariable association analyses between each of the clinicopahologic variables.

Abbreviations: SD, standard deviation; PC, plasma cell; HV, hyaline vascular; RI, resistance index.

3.2 Ultrasound performance of CD

The gray-scale ultrasound images obtained were all substantially hypoechoic masses, elliptical, with clear boundaries, complete envelope, uneven internal echo distribution, combined with branching, flocculent hyperechoic and/or point-like strong echoes, and most did not have an obvious lymphatic structure. Color Doppler ultrasound images manifest as abundant blood flow signals in the mass with lymphatic-like dendritic blood flow, or marginal basket-like blood flow, or a combination of the two blood flows. Blood flow classification: grade III to grade IV; spectral Doppler ultrasound images: the measured RI mean values were 0.57±0.05. All of the patients in the present study underwent fine needle aspiration before surgery, and all of the samples were considered to be hyperplasia

of lymphoid tissue with no clear diagnosis.

3.3 Gray ultrasound feature selection and ultrasonic signature building and validation

This study constructed a CD pathological type prediction method based on quantitative imaging omics. This study used a real clinical data set from the Department of US, Nanjing Hospital of Integrated Traditional Chinese and Western Medicine affiliated with Nanjing University of Traditional Chinese Medicine. The data set contained a total of 139 cases of CD US image data. After ROI segmentation, a total of 584 quantitative features of intensity, shape, texture, and wavelet features were extracted for each sample. Using the chi-square test and the PCA dimension reduction method, different feature spaces were selected to determine an optimized feature space with the highest prediction accuracy, and the feature space included 152 quantized image features. Then, the default data filling, normalization, and normalization processing were performed on the selected data. The corresponding CD pathological type prediction model was trained by the Gaussian Bayesian classification method, and the sensitivity, specificity, and accuracy of the model prediction were obtained; the degree was calculated. The overall accuracy of the model on the test set was 84.2%, the sensitivity was 90.1%, the area under the curve (AUC) was 0.925, and the specificity was 87.5%; the detailed data are listed in Tab. 2. Fig. 2 shows the P-R (precision-recall) diagram, and Fig. 3 is its receiver operating characteristic (ROC) curve.

Table 2: Diagnostic accuracy of predictive models of PC and HV types

Sensitivity (%)	Specificity (%)	Accuracy rate (%)
90.1	87.5	84.2
(10/11)	(7/8)	(16/19)

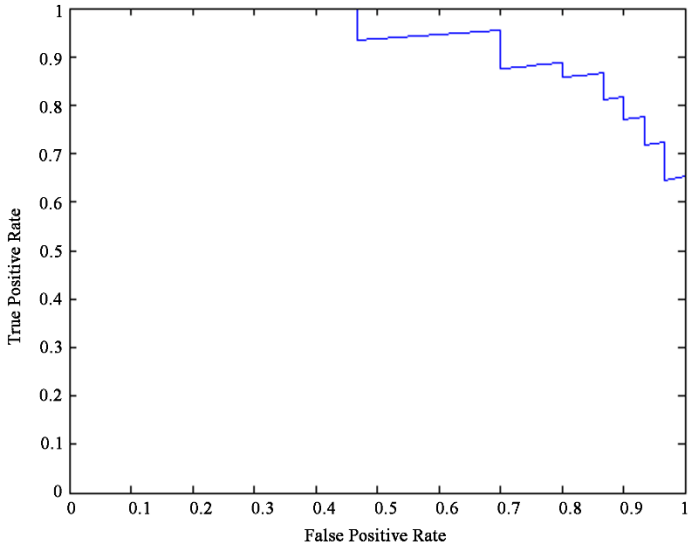

Figure 2: P-R diagram of feature prediction results

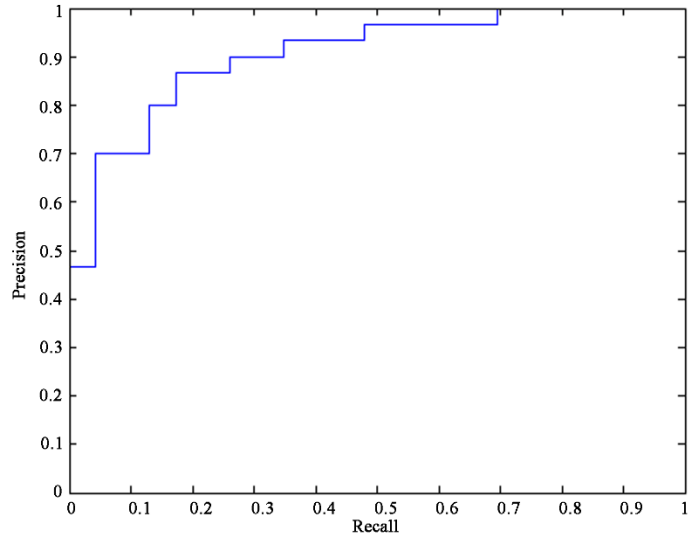

Figure 3: ROC diagram of feature prediction results

4 Discussion

Progress in ultrasound image analysis has always been fundamental to the advancement of image-guided intervention research due to the real-time acquisition capability of ultrasound, and this has remained true over the past two decades. In the present study, we present a novel, validated, and flexible US nomogram for quantitative image analysis using clinical

CD US data. Over all of the trials, our system achieved an accuracy of 84.2% and AUC of 0.925 for CD in predicting the presence of specific diseases. The US nomogram's accuracy is near that of expert readers for CD.

We propose that our framework could help nonexpert readers correctly classify CD US and flag images that are suspicious for CD that would otherwise be missed. Proper diagnosis prevents insignificant examination and treatment of the patient. Identifying CD earlier, especially PC-CD, could prevent the development of more severe symptoms and assist with obtaining disease treatment for a greater number of patients. Identifying at-risk cases of CD earlier could assist with treatment planning and parental counseling.

There is currently no corresponding classification application for CD, and therefore, this study can provide a satisfactory basis for computer-aided diagnosis of this disease. With the development of computer technology, and the rapid development of medical information in recent years, the digitization and big data of medical information have spawned research in the field of medical disease data analysis, which has made data classification an effective data analysis tool for auxiliary medicine. It plays an increasingly important role in clinical diagnosis, medical imaging, signal recognition, disease type classification, prognosis, gene microarray, and other applications. Due to the different sites of CD disease, clinical manifestations are diversified. Moreover, the clinical symptoms are not specific, and therefore, preoperative diagnosis is more difficult. Preoperative ultrasound examination will help to establish the presence of disease.

An ultrasound scan shows that the lesions are uniform in density, and the edges are smooth or are not soft tissue masses. The degree of enhancement of transparent vascular UCD lesions is slightly lower than that of adjacent large blood vessels, and the tumor is obviously strengthened due to the presence of additional blood vessels and abundant capillaries in the mass, while plasma cell UCD is less uneven due to less vascular components. Moderately enhanced, with a lack of characteristic performance, MCD has no obvious lumps in US findings, often showing lymph nodes with similar sizes in one or more regions, with mild to moderate enhancement [Han, Li and Zhang (2015); Linkhorn, van der Meer, Gruber et al. (2016); Wang and Hu (2007)]. In the latter two cases, imaging findings are atypical and preoperative diagnosis is difficult. The early diagnosis of this disease ultimately depends on histopathological examination.

In recent years, many researchers have carried out extensive and in-depth studies on medical image classification and mining, and the integration of new image classification methods and disease classification methods is also booming. There are many studies that combine image classification methods with disease classification to achieve better diagnostic results. For example, Alam et al. [Alam, Lizzi, Feleppa et al. (2002)] developed a classification diagnostic system for benign malignant breast lesions on ultrasound images using echogenicity, inhomogeneity, shadow, area, aspect ratio, edge irregularity, and boundary resolution. To obtain quantitative acoustic features, they used sliding window Fourier analysis to calculate spectral parameter maps of radio frequency (RF) echo signals in lesions and adjacent regions, and quantified morphological features by tracking geometric and fractal analyses of lesion boundaries. They analyzed data obtained during routine ultrasound examination of 130 biopsy regular patients, and the operating characteristic area of the subject under the curve was 0.947 ± 0.045. The basic data for 50

patients with lung cancer and the digital features of X-ray films were used to expose a rough set to feature data mining, which greatly improved the accuracy of the early diagnoses of lung cancer patients [Kusiak, Kemstine and Kem (2000)]. Various types of breast image data were extracted from the medical image database [Antonie, Zaiane and Coman (2001)]. Association rules and neural networks are used to mine the texture features of different regions, which effectively realizes automatic diagnosis for breast cancer patients, that is, positive abnormal classification. This resulted in a new situation for subsequent medical image classification research. Using decision trees, the underlying visual features of the image and the diagnostic information from clinical experts are mined, and the implicit associations assisted clinicians in medical diagnosis [Petra (2002)]. This is a simple and fast classification method. Since then, many researchers have used the decision tree algorithm to classify and diagnose breast diseases, and have made continuous improvements to the algorithm. The logistic regression analysis (LRA) algorithm was used to discover the relationship between brain and finger movements and words and deeds [Kakimoto, Morita and Tsukimoto (2000)]. In the classification of breast cancer, neural networks and association rules were used for mining, and comparative analysis showed that the neural network method is less sensitive to data set imbalance than the association rule mining method [Zaiyane, Antonie and Coman (2002)]. In 2002, breast tumors were classified using wavelet transform and neural networks [Chen, Chang, Kuo et al. (2002)]. In 2007, support vector machine (SVM)-based classification of cervical lymph nodes, such as size and shape features, was proposed [Zhang, Wang, Dong et al. (2007)]. This method is applicable to two types of problems. At present, new progress has been made in the research and application of medical image mining. The retina was studied using an artificial neural network [David, Krishnan and Kumar (2008)]. Additionally, a neural network was used to classify the brain images of patients with Alzheimer's disease [Ramírez, Chaves, Górriz et al. (2009)]. The results showed that it is helpful for the diagnosis of early Alzheimer's disease.

Researchers have achieved certain results in the classification of medical images. However, it is difficult to quickly and accurately detect or distinguish lesions in medical images with unclear sampling periods, various sample types, different characteristics, high dimensionality, and large data volume for analysis, calculation, and extraction. Effectively characterizing the content and mining additional valuable information still has broad research and application prospects.

The results of this study showed that the addition of clinical factors significantly improved the classification accuracy of the constructed ultrasoundomics nomogram. The likely reason is that the ultrasound characteristics of CD are easily confused with the ultrasound phenotype of other superficial diseases. An example is lymphoma, which is also more common in young adults, and is early local, late in the systemic stage, often accompanied by systemic symptoms, such as fever, hepatosplenomegaly, and systemic lymphadenopathy. The difference with CD is that cystic changes and calcification are rare before the treatment of swollen lymph nodes, the blood flow inside the lymph nodes is rich, and the blood supply of the lymph nodes is dendritic, while the blood flow distribution in UCD disease is surrounded by a mixed blood supply. Lymph node tuberculosis is also a young adult disease with a long disease course. The mass is hard, and it is characterized by a cluster of lymph nodes, fusion, unclear borders, and internal echoes. Some lesions are

accompanied by abscesses and sinuses. The difference with CD is that the ultrasound image of lymph node tuberculosis is lumpy and there is patchy calcification, while the UCD calcification is punctate, branched hyperechoic, or with strong echo. Paraganglioma, like CD, is rich in dilatation and distortion of blood vessels, but often grows along the aorta, and UCD is often distributed according to the lymphatic chain. Schwannoma, which also occurs in young adults, is a painless mass, and the tumor activity is related to the direction of the nerve. Generally, it can only move up and down the long axis, and clinical symptoms and nerve sources are closely related. Carotid body tumors have their specific pathological sites, and clinical lumps have a pulsating sensation, with the characteristics of the widening of the bifurcation of the internal and external carotid arteries. Carotid angiography can confirm the diagnosis. Most of the metastatic cancers have a history of primary tumors, and the internal echoes of the lesions are uniform or uneven. They may be necrotic and liquefied, partially merged with each other, and even surround adjacent tissues. The papillary metastases of thyroid cancer often have microcalcification. Therefore, adding some clinical data can improve the accuracy of the classification results.

Although this study is helpful for computer-aided diagnosis of CD, as with many other imaging omics studies, the application of imaging omics to clinical diagnosis is still in its early stages, and many process details of imaging omics are subject to research and improvement. First, the imaging devices from different manufacturers have different degrees of image acquisition, reconstruction algorithms and parameter settings, and there is no uniform standard. Even if the same device is used, the patient's cooperation will have a potential impact on the ultrasound image data of mass. Second, in addition, the accuracy of the imaging ensemble model prediction is related to the number of features, feature screening methods, and classifiers. Therefore, the most optimal features are selection and mode. The identification method needs to be further explored. Third, there is currently no research on the application of imaging omics in CD, and there are few studies that can provide references for this research. Finally, imaging omics is an interdisciplinary subject, and engineering researchers need to work with imaging physicians to complete the overall work of imaging omics.

5 Conclusion and forecast

Although this study was able to successfully classify HV and PC based on ultrasound images and clinical characteristics, and to achieve the same classifications as those of experienced clinicians, there are still some limitations. First, the ROI used in the ultrasonic image processing was manually drawn by humans. There were some differences between the results of different operators when manually delineating the ROI. These factors will bias the measurement of the image omics characteristics. In this way, the classification effect of our ultrasonic nomogram will be very dependent on the choice of the ROI, and it is also very time consuming. Therefore, the ability to automatically segment these ROIs can improve the classification and efficiency for our models. Secondly, there are three types of CD pathology: HV, PC, and mixed type. In the current study, we did not consider the mixed type of CD. However, different CD pathological types correspond to different treatment methods for diseases. Therefore, our later work will mainly focus on the classification of all three CD pathological types [Meng, Rice, Wang et al. (2018)], if

sufficient pathological data can be obtained. Finally, our sample size is small and the source is single, which challenges the stability and universality of our model. Additional clinical sample data need to be included.

Ethics statement

This study was carried out in accordance with the recommendations of the Institutional Review Board of Nanjing Hospital of Integrated Traditional Chinese and Western Medicine with written informed consent from all subjects. All of the subjects gave written informed consent in accordance with the Declaration of Helsinki.

Conflicts of interest statement

The authors declare that they have no conflicts of interest regarding the publication of this paper.

Acknowledgement: This work was supported by the National Natural Science Foundation [grant number 61806029]; the Chengdu University of Information Engineering Research Fund [grant number KYTZ201719]; Youth Technology Fund of Sichuan Provincial Education Hall [grant number 17QNJJ0004]; and the Project of Sichuan Provincial Education Hall [grant numbers 18ZA0089, 2017GZ0333 and 2018Z065]. We thank LetPub (www.letpub.com) for its linguistic assistance during the preparation of this manuscript.

References

Alam, S. K.; Lizzi, F. L.; Feleppa, E. J.; Liu, T.; Kalisz, A. (2002): Computer-aided diagnosis of breast lesions using a multifeature analysis procedure. *Proceedings of SPIE-The International Society for Optical Engineering*, vol. 4687, pp. 296-303.

Antonie, M. L.; Zaiane, O. R.; Coman, A. (2001): Application of data mining techniques for medical image classification. *MDM/KDD with ACM SIGKDD Conference*.

Bucher, P.; Chassot, G.; Zufferey, G.; Ris, F.; Huber, O. et al. (2005): Surgical management of abdominal and retroperitoneal Castleman's disease. *World Journal of Surgical Oncology*, vol. 3, no. 1, pp. 1-9.

Chen, D. R.; Chang, R. F.; Kuo, W. J; Chen, M. C.; Huang, Y. L. (2002): Diagnosis of breast tumors with sonographic texture analysis using wavelet transform and neural networks. *Ultrasound in Medicine & Biology*, vol. 28, no. 10, pp. 1301-1310.

David, J.; Krishnan, R.; Kumar, A. (2008): Neural network based retinal image analysis. *Congress on Image and Signal Processing*, vol. 2, pp. 49-53.

Frizzera, G. (1988): Castleman's disease and related disorders. *Seminars in Diagnostic Pathology*, vol. 5, no. 4, pp. 346-64.

Hacihaliloglu, I. (2017): Ultrasound imaging and segmentation of bone surfaces: a review. *Technology (Singap World Scientific)*, vol. 5, no. 2, pp. 74-80.

Han, H.; Li, X.; Zhang, B. (2015): Clinical pathological analysis of Castleman disease and literature review. *Journal of Clinical and Experimental Pathology*, vol. 31, no. 1, pp. 4.

Kakimoto, M.; Morita, C.; Tsukimoto, H. (2000): Data mining from brain image.

Proceedings of the International Workshop on Multimedia Data Mining, pp. 91-97.

Kusiak, A.; Kemstine, K. H. K.; Kem, J. A. (2000): Data mining: medical and engineering case studies. *Proceedings of the Industrial Engineering Research 2000 Conference*, pp. 7.

Lambin, P.; Rios-Velazquez, E.; Leijenaar, R.; Carvalho, S.; van Stiphout, R. G. P. M. et al. (2012): Radiomics: extracting more information from medical images using advanced feature analysis. *European Journal of Cancer*, vol. 48, no. 4, pp. 441-446.

Linkhorn, H.; van der Meer, G.; Gruber, M.; Mahadevan, M. (2016): Castleman's disease: An unusually young presentation resulting in delayed diagnosis of a neck mass. *International Journal of Pediatric Otorhinolaryngology*, vol. 86, pp. 90-92.

Ma, Q.; He, W. (2013): Advances in clinical and imaging studies of Castleman's disease. *Shanxi Medical Journal*, vol. 42, no. 3, pp. 149-150.

Meng, R.; Rice, S. G.; Wang, J.; Sun, X. (2018): A fusion steganographic algorithm based on faster R-CNN. *Computers, Materials and Continua*, vol. 55, no. 1, pp. 1-16.

Nu, M. Q.; Liu, H.; Diss, T. C. (2001): Kaposi sarcoassociated herpes virus infects monotypic (IgM lambda) but polyclonalnave B cells in Castleman disease and associated lymphoproliferative disorder. *Bloof*, vol. 97, no. 7, pp. 7.

Petra, P. (2002): Image mining: issues, framework, a generic tool and its application to medical-image diagnosis. *Engineering Applications of Artificial Intelligence*, vol. 15, no. 2, pp. 205-216.

Ramírez, J.; Chaves, R.; Górriz, J. M.; Álvarez, I.; López, M. et al. (2009): Functional brain image classification techniques for early Alzheimer disease diagnosis. *International Work-Conference on the Interplay Between Natural and Artificial Computation*, pp. 150-157.

Schneider, C. A.; Rasband, W. S.; Eliceiri, K. W. (2012): NIH image to ImageJ: 25 years of image analysis. *Nature Methods*, vol. 9, no. 7, pp. 671-675.

Soumerai, J. D.; Sohani, A. R.; Abramson, J. S. (2014): Diagnosis and management of Castleman disease. *Cancer Control*, vol. 21, no. 4, pp. 266-78.

Wang, D.; Hu, C. (2007): Imaging diagnosis of Castleman's disease. *Journal of Suzhou University: Medical Science*, vol. 27, no. 3, pp. 466-467.

Xuan, W. (2015): *Superficial Tissue Ultrasound and Pathological Diagnosis*. People's Military Medical Press.

Zaiyane, O. R.; Antonie, M.; Coman, A. (2002): Mammography classification by an association rule-based classifier. *International Workshop on Multimedia Data Mining*.

Zhang, J.; Wang, Y.; Dong, Y.; Wang, Y. (2007): Ultrasonographic feature selection and pattern classification for cervical lymph nodes using support vector machines. *Computer Methods and Programs in Biomedicine*, vol. 88, no. 1, pp. 75-84.

Zhang, J.; Wang, Y.; Dong, Y. (2008): Evaluation of ultrasound image feature extraction of cervical lymph nodes. *Journal of Biomedical Engineering*, vol. 25, no. 1, pp. 5.